J Therm Anal Calorim (2014) 117:101–108
DOI 10.1007/s10973-014-3662-1

The revised phase diagram of the $Ca_3(PO_4)_2$–YPO_4 system. The temperature and concentration range of solid-solution phase fields

Aleksandra Matraszek · Ewa Radomińska

Received: 30 August 2013 / Accepted: 15 January 2014 / Published online: 9 February 2014

Abstract A revised version of the $Ca_3(PO_4)_2$–YPO_4 phase diagram has been proposed on the basis of results obtained by thermal analysis (DTA/DSC/TG) and X-ray diffraction methods. A limited solid solution with the structure of β-$Ca_3(PO_4)_2$ exists in the system. At 1,100 °C the maximal concentration of YPO_4 in the solid solution is ~15 mass%. The solid-solution phase field exists in the temperature range upto ~1,380 °C. Two high-temperature solid solutions with the structure of α′ and α-$Ca_3(PO_4)_2$ form in system as well, however only the α phase can be obtained by quenching from high temperatures. The $Ca_3Y(PO_4)_3$ compound with the structure of eulytite forms in the $Ca_3(PO_4)_2$–YPO_4 system at temperatures exceeding 1,255 °C and does not show any polymorphic transition.

Keywords Calcium phosphate · Rare earth compounds · Phase diagram · Thermal analysis · X-ray diffraction

Introduction

Calcium phosphates have aroused much interest as bioactive compounds. They are used as components of different kinds of materials applied in dental and orthopedic surgery [1, 2].

Among other bioactive calcium compounds, tricalcium bis(phosphate), $Ca_3(PO_4)_2$, is one of the most interesting materials. It melts congruently at a high temperature (T_m = 1,810 °C) [3], and it has three polymorphic modifications: β, α, and α′. The α′ form exits at temperatures above 1430 °C [4] and it has a trigonal structure (S.G $P\bar{3}m$) with parameters: $a = b = 5.3507(8)$, $c = 7.684(1)$ Å [5]. It is not possible to overcool the polymorph, even in the course of quenching.

The α-$Ca_3(PO_4)_2$ form is stable in a temperature range of 1,125–1,430 °C [6–8] and has a monoclinic structure with a $P2_1/a$ space group [5, 9]. The biodegradation and bioreabsorption processes of α-$Ca_3(PO_4)_2$ occur in physiological environment faster than that of hydroxyapatite and β-$Ca_3(PO_4)_2$. This makes the α-phase suitable for application as osteoconductive material and/or biodegradable drug carrier [10, 11].

At temperatures below 1,125 °C exists the low-temperature β-$Ca_3(PO_4)_2$ form, which is characterized by a trigonal structure with unit cell parameters: $a = b = 10.4352(2)$ Å, $c = 37.4029(5)$ Å [12]. The structure of the phase is complicated: there are five cationic sites with coordination number relative to oxygen from 3 to 8. In pure β-$Ca_3(PO_4)_2$ or doped with divalent cations one of the Ca sites is half occupied [13, 14]. The same Ca position is empty for RE^{3+} doping, which is associated with charge balance mechanism [15, 16]. This feature of the structure makes the β-$Ca_3(PO_4)_2$ phase a perfect host lattice for doping with mono-, di-, and/or trivalent cations. The wide range of dopants and doping concentrations enables modification of physicochemical properties of $Ca_3(PO_4)_2$. The β-$Ca_3(PO_4)_2$-derived phases show optical activity [17–20], are considered as bioceramics or biocements [21–26] and show interesting electric properties [27–29].

The β→α structural change has a reconstructive character. This implies that a long-term heating at a

Electronic supplementary material The online version of this article (doi:10.1007/s10973-014-3662-1) contains supplementary material, which is available to authorized users.

A. Matraszek (✉) · E. Radomińska
Department of Inorganic Chemistry, Faculty of Engineering and Economics, Wrocław University of Economics, Komandorska 118/120, 53-345 Wrocław, Poland
e-mail: aleksandra.matraszek@ue.wroc.pl

temperature above the phase transition point is necessary to complete the β→α transformation. The process is reversible, however due to the high activation energy of the α→β transformation the monoclinic form of $Ca_3(PO_4)_2$ does not revert to the low-temperature form, when cooled with moderate cooling rate (5 °C min^{-1}) [8, 30].

The thermodynamically stable form of YPO_4 is of xenotime type with structural parameters of tetragonal elementary cell (S.G. I41/amd): $a = 6.8840(3)$, $c = 6.0202(3)$ Å [31]. It is refractory material with a melting point at 1,995 ± 20 °C [32] or 2,150 °C [33].

Phase diagrams of phosphate systems with rare earth elements have been studied by our group in last decades [34–39]. In the $Ca_3(PO_4)_2$-*RE*PO_4 systems (*RE* = Y, La, Ce) form compounds with the formula $Ca_3RE(PO_4)_3$ [34–36]. They exist only at high temperatures and have a regular structure of eulytite (S.G. $I\bar{4}3d$) [40, 41]. It has been also reported that the $Ca_3Y(PO_4)_3$ phase has a complicated thermal behavior. According to Ref. [34] the phosphate melts congruently at 1,790 °C and at temperatures below 1,215 °C it decomposes to YPO_4 and $Ca_3(PO_4)_2$. In addition, the compound has a reversible β→α polymorphic transition at 1,255 °C. The $Ca_3Y(PO_4)_3$ phase forms with $Ca_3(PO_4)_2$ and YPO_4 two eutectic systems with melting temperature at 1,684 and 1,674 °C, respectively. The $Ca_3Y(PO_4)_3$ phase can be quenched to room temperature, however, during heating/cooling with rate of 40–400 °C min^{-1} occurs a martensitic transformation [41].

In the $Ca_3(PO_4)_2$-*RE*PO_4 systems (*RE* = La, Ce, and Eu) fields of limited solid solution with the structure of β–$Ca_3(PO_4)_2$ were found [16, 35, 36]. In contrast to the results, the study of the phase relationships in the $Ca_3(PO_4)_2$–YPO_4 system did not consider existence of any type of solid solution [34]. The comparison of the most recent phase equilibria studies of systems with $Ca_3(PO_4)_2$ implies that the phase relationships in the $Ca_3(PO_4)_2$–YPO_4 system are more complicated as presented in the Ref. [34]. Because of an growing interest on materials derived from $Ca_3(PO_4)_2$ and doped with rare earth elements, a revision of the $Ca_3(PO_4)_2$–YPO_4 system has been undertaken. The aim of the present research was to clarify the divergences between reported studies with the attention focused on thermal and concentration range of solid-solution phase fields, as well as on the polymorphism of the $Ca_3Y(PO_4)_3$ eulytite phase.

Experimental

Synthesis

The following analytical reagents were used to obtain the $Ca_3(PO_4)_2$ compound: $CaCO_3$, $CaHPO_4$ (analytical grade, POCh Gliwice). The phosphate was prepared in a solid state by the ceramic method according to method proposed in [42]. In this synthesis route, a stoichiometric mixture of $CaCO_3$ and $Ca_2P_2O_7$ was annealed at 900 °C for 5 h, which was followed by grinding in an agate mortar and heating for 5 h at 1,400 °C. The $Ca_2P_2O_7$ compound was prepared from $CaHPO_4$ by calcination at 900 °C (2 h).

The YPO_4 was obtained by precipitation from a suspension of Y_2O_3 (99.99 %, POCh, Poland) in diluted H_3PO_4 (85 %, POCh Gliwice). The molar ratio of $[PO_4^{3-}]$:$[Y^{3+}]$:H_2O was 1:0.023:25. The suspension was boiled under reflux for at least 6 h. The obtained precipitate was filtered and washed with hot distilled water. Finally, the powder was calcined at 1,400 °C for 2 h to expel moisture and adsorbed pyrophosphates.

The binary samples of the $\{(100–x)Ca_3(PO_4)_2 + x\text{-}YPO_4\}$ composition, where $x \leq 50$ (*x*—the mass% of YPO_4), were synthesized by carefully grinding of a mixture of $Ca_3(PO_4)_2$ and YPO_4. The chemical composition of samples under study is shown in the Tab. S1 (supplementary material). The powders were pelletized, preliminary heated at 900 °C for 10 h, and finally at 1,100 °C for 40 h in several heating steps. Between the stages samples were quenched, ground, and homogenized in an vibratory mill (Fritsch, Pulverisette 23) in isopropanol. The phase composition of samples was examined by X-ray diffraction (XRD) method. The same results of XRD measurements after two annealing steps were a prove that equilibrium state had been reached.

The $Ca_3Y(PO_4)_3$ eulytite was obtained from $Ca_2P_2O_7$ and Y_2O_3. The ground and pelletized mixture of the reagents was quenched after sintering stage at 1,400 °C for 10 h.

The samples were quenched from high temperatures (above 1,400 °C) as follows: the pelletized powders were closed in welded ampoules made of Pt30Rh and after appropriate heating steps dropped into a mixture of water and ice from a vertical tubular furnace.

Characterization methods

The DTA/TG experiments were carried out using Derivatograph 3427 (MOM, Hungary). The samples were heated in a temperature range of 20–1,450 °C (heating rate: 7.5 °C min^{-1}, Pt crucible, sample mass 450–600 mg, air atmosphere). The temperature calibration factor for the thermal experiments was obtained at the phase transition temperature of K_2SO_4 (583 °C), its melting point (1,070 °C) and the melting point of $Ca_2P_2O_7$ (1,353 °C).

Phase analysis of the samples was made using XRD technique and a Siemens D5000 diffractometer equipped with a Cu X-ray tube. The measurements were performed in 2θ range of 5–80° with a 0.02° step and at least 4 s per

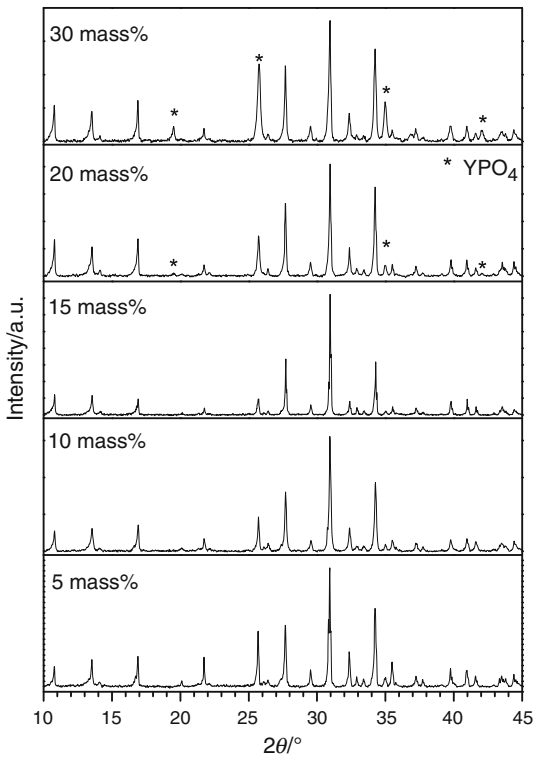

Fig. 1 The XRD patterns of samples with different YPO_4 concentration. Samples were obtained by quenching from 1,100 °C

step. Silicon (99.995 % ABCR GmbH) was used as an external standard for refinement of structural parameters. Lattice constants of the β-$Ca_3(PO_4)_2$ unit cell were refined using Checkcell software [43].

Results and discussionwec

Phase equilibria study

The phase composition of samples sintered at selected temperatures was obtained by the XRD measurements. In the diffraction patterns of samples sintered at 1,100 °C the main phase was β-$Ca_3(PO_4)_2$ (Fig. 1). The YPO_4 phase was found in samples with $x(YPO_4) \geq 20$ mass%. It should be also mentioned that several of the most intensive YPO_4 reflections overlapped with these of β-$Ca_3(PO_4)_2$. This made the qualitative analysis of the patterns complicated. The SEM study of the samples confirmed that the samples with $x > 25$ mass% are biphasic. In the Fig. 2 are shown the BSE images of samples with $x(YPO_4) = 15$–30 mass%. The sample with the lowest content of YPO_4 has a single-phase character (Fig. 2a). In the images of samples with $x = 25$ and 30 mass% secondary grains of light color are visible (Fig. 2b, c). The light color of grains is connected with high concentration of yttrium (element with high mass number). Unfortunately, the yttrium L line (1.922 keV) is very close to the P(K) absorption edge (2.013 keV). Since the lines overlap, the accurate determination of Y concentration in samples containing both elements (yttrium and phosphorus) can be not determined.

The lattice constants of the β-$Ca_3(PO_4)_2$ unit cell for samples with the $x \leq 25$ mass% were refined using the Checkcell software on basis of the β-$Ca_3(PO_4)_2$ phase parameters reported in [13]. The change of the obtained lattice constants versus molar fraction of YPO_4 is shown in Fig. 3 and the values are shown in Table 1. There is an evident decrease of c parameter value in the concentration range of 0–15 mass% (0–23 mol%) and according to the Vegard's rule in the range exits the limited solid solution of YPO_4 in β-$Ca_3(PO_4)_2$. The ionic radius of yttrium (1.02 Å) is smaller than that of calcium 1.12 Å [44] and hence the exchange of yttrium for calcium ions in the structure of β-$Ca_3(PO_4)_2$ results in a decrease of the solid solution unit cell volume (Table 1).

The chemical composition of the obtained solid solution can be expressed by the formula: $Ca_{3-3z}Y_z(PO_4)_{2-z}$, where z is the molar fraction of YPO_4. Yttrium is introduced into the structure of β-$Ca_3(PO_4)_2$ with simultaneous formation of vacancy according to the scheme: $3Ca^{2+} \rightarrow 2Y^{3+} + \square$ [15, 16]. It has been stated in Refs. 15–17 that the maximal $REPO_4$ concentration in the β-$Ca_3(PO_4)_2$ solid solution should not exceed 25 mol%. The maximal RE concentration is connected with the fact that at that point, the smallest and irregular Ca site is completely vacant [16, 17].

The phase composition of samples quenched from 1,400 °C was depended on mass content of YPO_4. The Fig. 4 presents the XRD patterns of samples with $x \leq 12$ mass% of YPO_4 heated at the temperature.

In the sample with 2.4 mass% of YPO_4 reflections of only α-$Ca_3(PO_4)_2$ have been found. The same phase composition has been found by XRD for the sample quenched from 1,600 °C. The pellets quenched from high temperatures were cracked, which was a sign of transitions occurring in the material. In order to obtain the sample with $x(YPO_4) = 2.4$ mass% in the α structure, quenching from high temperatures was necessary. The same powders cooled in an electric furnace with moderate cooling rate were characterized by the presence of only β phase. This finding is in contradiction with the metastable character of the overcooled α form in the $Ca_3(PO_4)_2$–$Mg_3(PO_4)_2$ system [8]. The authors of the manuscript stated that quenching is not required to retain the α phase on cooling.

The preparation with $x = 5$ mass% of YPO_4 was diphase; both α and β-$Ca_3(PO_4)_2$ phase reflections were identified in the XRD pattern (Fig. 4). The diffractogram of

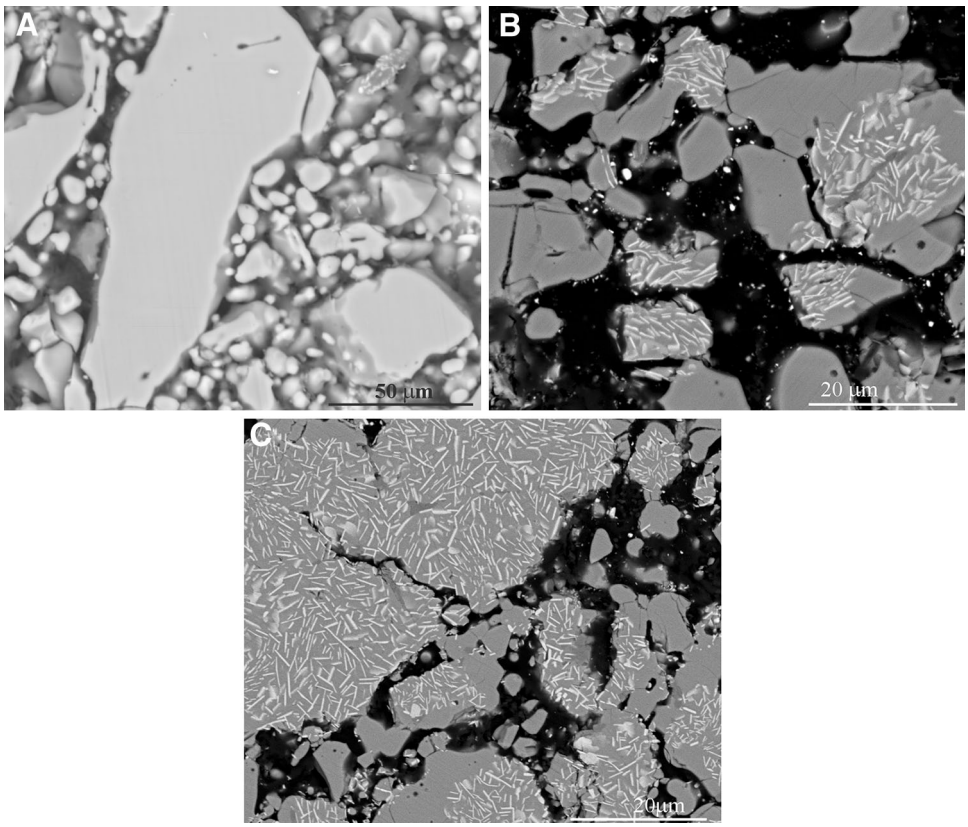

Fig. 2 The SEM images (the BSE mode) of samples quenched from 1,100 °C. Sample with $x(YPO_4) = 15$ (**a**), 25 (**b**), and 30 mass% (**c**)

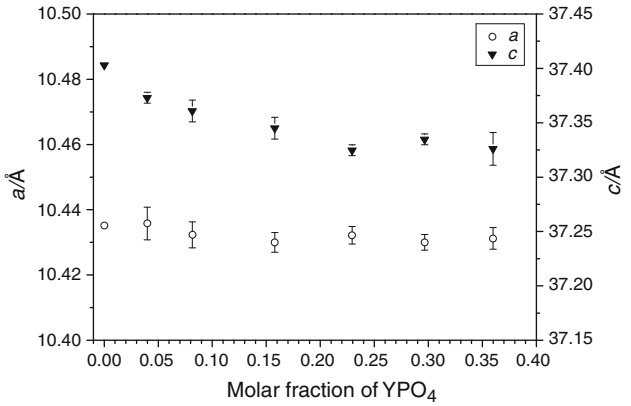

Fig. 3 The unit cell parameters of the solid solution of YPO_4 in β-$Ca_3(PO_4)_2$ versus molar fraction of YPO_4

Table 1 The lattice parameters of $Ca_{3-3z}Y_z(PO_4)_{2-z}$ solid solution in samples heated at 1,100 °C for 40 h and quenched in ice

Molar fraction of YPO_4/z	a/Å	c/Å	V/Å^3
0.0398	10.436(5)	37.373(5)	3524.8(8)
0.0815	10.432(4)	37.361(10)	3521.3(8)
0.1578	10.430(3)	37.345(10)	3518.3(9)
0.2294	10.432(3)	37.325(5)	3517.9(9)
0.2966	10.430(2)	37.335(5)	3517.3(10)
0.3599	10.431(3)	37.326(15)	3517.3(8)

the sample quenched from 1,600 °C did not show considerable changes. On the DTA curve of the powder, three endothermic effects were registered at 1305, 1375, and 1420 °C.

The powders with $10 < x < 50$ sintered at 1,400 °C were biphasic and contained β-$Ca_3(PO_4)_2$ solid solution and $Ca_3Y(PO_4)_3$ phosphate.

The presence of the β phase in the samples quenched from high temperatures was surprising, since the α/α′-$Ca_3(PO_4)_2$ solid solutions formation has been evidenced in the sample with the lowest YPO_4 content. As mentioned above, on the DTA curves of the powders with the low YPO_4 content, thermal effects connected to phase transitions have been observed. The presence of the β form instead of the α (or α′) solid solution could be explained by the probable lower energy barrier of the α→β transition occurring on cooling in the $Ca_3(PO_4)_2$ solid solutions in comparison to the undoped $Ca_3(PO_4)_2$. Since the high-energy barrier stabilizes the metastable α phase at room temperature, its lowering should result in rapid transition and presence of the low-temperature solid solution in samples quenched from high temperatures. At the same

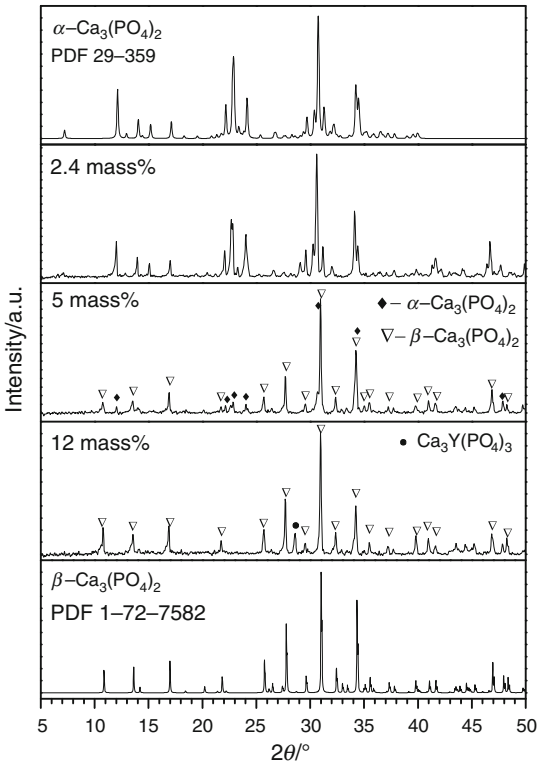

Fig. 4 The XRD patterns of samples with different YPO_4 concentration quenched from 1,400 °C

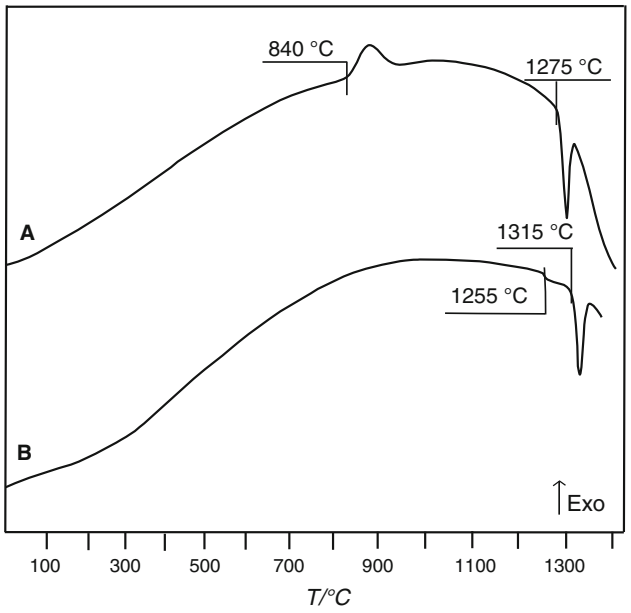

Fig. 5 The DTA curves of heating of $Ca_3Y(PO_4)_3$ compound obtained by quenching from 1,400 °C (*a*) and the same sample subjected to heating 20 h at 1,100 °C (*b*)

time, the α' modification of $Ca_3(PO_4)_2$ could be not obtained by quenching [4].

Thermal behavior of $Ca_3Y(PO_4)_3$

The $Ca_3Y(PO_4)_3$ phosphate belongs to phases existing at high temperatures. Presence of the compound was identified only in samples quenched from temperatures above 1,255 °C. In the present study, the phase pure compound has been obtained by reacting of $Ca_2P_2O_7$ and Y_2O_3 at 1,400 °C. In the previously published studies [35, 36, 45] it has been shown that the most effective route to obtain phase pure $Me_3RE(PO_4)_3$ phases is the application of more reactive substrates, for instance $Me_2P_2O_7$ and *RE* oxides. This eliminates the problem with the relative slow eulytite formation, which is dependent on diffusion processes occurring upon β-$Ca_3(PO_4)_2$ solid solution decomposition. In addition, quenching from high temperatures (above of ~1,250 °C) is necessary to obtain single-phase powders. When quenched, the $Me_3RE(PO_4)_3$ phases show metastable character, since slow diffusion in bulk at room temperature stops the decomposition of the compound.

The thermal behavior of phase pure $Ca_3Y(PO_4)_3$ was studied by DTA (Fig. 5a) and XRD (Fig. 6) techniques. On the heating curve of the compound quenched from 1,400 °C two thermal effects were identified: exothermic

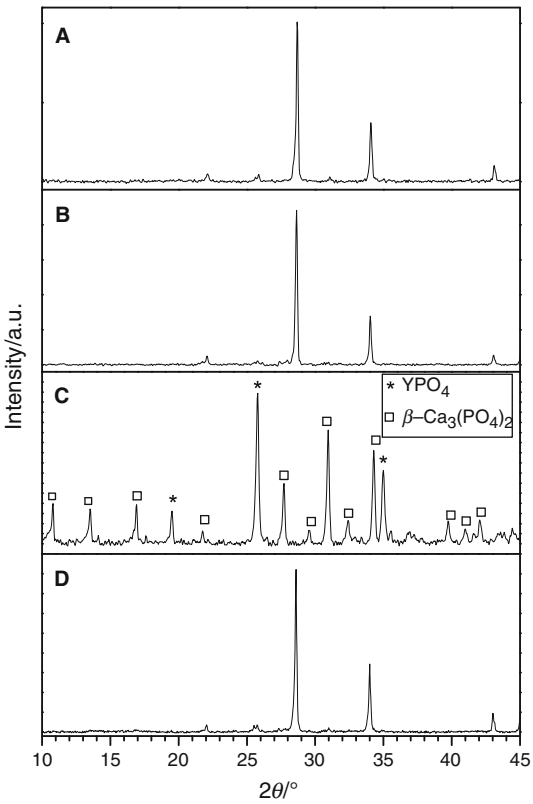

Fig. 6 The XRD patterns of $Ca_3Y(PO_4)_3$ compound obtained at 1,400 °C (*a*) and the same sample after heating at 400 °C (*b*), 1,240 °C (*c*), and 1,285 °C(*d*)

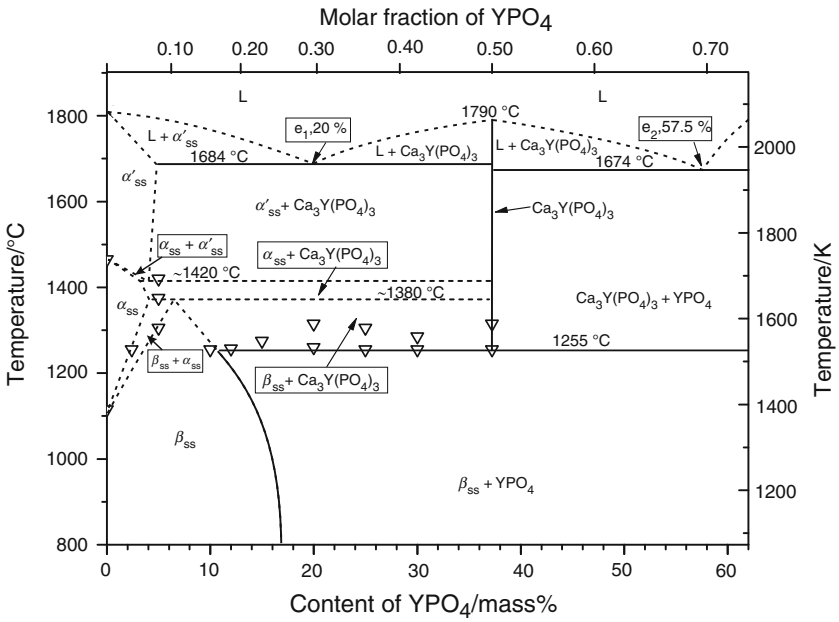

Fig. 7 The phase diagram of the $Ca_3(PO_4)_2$–YPO_4 system. The abbreviations α'_{ss}, α_{ss}, and β_{ss} denote, respectively, α', α, and β-$Ca_3(PO_4)_2$ solid solutions. [∇–onset temperatures of endothermic effects registered on DTA heating curves]

and endothermic one at, respectively, 840 and 1,275 °C (Fig. 5a).

The single-phase powder (consisting of eulytite phase only) subjected to 20 h heating at 1,100 °C was biphasic (Fig. 6c). It composed of a mixture of β-$Ca_3(PO_4)_2$ solid solution and YPO_4 and showed a slightly different thermal behavior (Fig. 5b). No exothermic effects were observed on the DTA curve, however, two endothermic effects were recognized: one broad and weak peak at ~1,255 °C and one strong effect at 1,315 °C.

The XRD patterns of the $Ca_3Y(PO_4)_3$ sample heat treated at different temperatures (Fig. 6) helped to explain the observed thermal effects. The $Ca_3Y(PO_4)_3$ compound has been found in powders quenched from 1,400 and 1,285 °C (Fig. 6a, d). Heating of the phase pure phosphate at a temperature below 840 °C, i.e., below the temperature of the exothermic effect, did not change the phase composition of the powder, it remained single phase (Fig. 5b). The same powder quenched from 1,100 and 1,240 °C was biphasic and composed of a mixture of YPO_4 and β-$Ca_3(PO_4)_2$ solid solution (Fig. 6c). From the results of the XRD study, it can be concluded that the formation point of $Ca_3Y(PO_4)_3$ lies between 1,240 and 1,285 °C and the metastable phase decomposes at temperature range 840–1,255 °C.

Summarizing, the thermal effects visible on the DTA heating curves of $Ca_3Y(PO_4)_3$ (Fig. 5) can be attributed to following processes:

– decomposition of the overcooled (metastable) $Ca_3Y(PO_4)_3$ phase into the β-$Ca_3(PO_4)_2$ solid solution and YPO_4 at ~840 °C (the exothermic effect in Fig. 5a);
– crystallization of the $Ca_3Y(PO_4)_3$ phase from parent phosphates taking place in a temperature range (the endothermic effects on both DSC curves in the temperature range 1,255–1,315 °C).

The onset temperature of the first endothermic effect (1,255° C) was chosen as the starting point of the compound synthesis from YPO_4 and β-$Ca_3(PO_4)_2$ solid solution. The formation of $Ca_3Y(PO_4)_3$ occurs with difficulties at this temperature because it is accompanied by a significant change in the chemical composition of the solid solution being in equilibrium. Above 1,255 °C the $Ca_3Y(PO_4)_3$ compound should be regarded as a thermodynamically stable phase.

The observed thermal behavior of the $Ca_3Y(PO_4)_3$ compound is similar to that of the $Ca_3Ce(PO_4)_3$ and $Sr_3Ce(PO_4)_3$ phases [36, 45]. The phases can be quenched from temperatures exceeding their formation point and they are metastable present at room temperature. Upon heating of the metastable phases at a moderate temperature (upto ~800 °C) the decomposition of the phosphates is stopped, by kinetic hindrances. First at ~800 °C starts the decomposition, which manifests on DTA curves in form of exothermal effects. Above the temperature, the powders can attain the equilibrium state. Under further heating YPO_4 and β-$Ca_3(PO_4)_2$ solid solution react at a temperature above of 1,255 °C, which results in formation of the eulytite-type phase. The synthesis of the high-temperature phosphate is accompanied by a registration one or two endothermic effects on the DTA heating curves. The same thermal behavior has been registered for the $Ca_3Ce(PO_4)_3$ phase [36].

It has been shown in [34] that the $Ca_3Y(PO_4)_3$ phosphate forms at 1,215 °C and has a polymorphic transition at 1,255 °C. In contrast to the statement, it has been above revealed that the compound is not a stable phase at 1,240 °C. In addition, in Refs. [38, 45] it has been shown that the thermal effects connected to the formation/decomposition of $Me_3RE(PO_4)_3$ are characterized by a large thermal hysteresis. The difference between the onset temperatures of effects on heating and cooling DTA curves is connected to kinetic hindrances occurring by the decomposition/formation of new phases and is a sign of reconstructive-type transformations [45, 46]. Because the experiments presented in [34] were carried out in cooling runs, the most probably the effects at 1,215 and 1,255 °C were both connected to the decomposition of $Ca_3Y(PO_4)_3$.

The phase diagram of the $Ca_3(PO_4)_2$–YPO_4 system

On basis of results of the XRD and DTA study, it was possible to propose a revised version of the $Ca_3(PO_4)_2$–YPO_4 phase diagram (Fig. 7). The figure summarizes all onset temperatures of the endothermic effects registered during the DTA heating runs of samples sintered at 1,100 °C. The temperature and composition of eutectic points, as well as the melting point of $Ca_3Y(PO_4)_3$ have been adopted from [34]. The melting point of $Ca_3(PO_4)_2$ has been taken from [3].

There are three solid-solution phase fields. The composition range of the limited solid solution of YPO_4 in β-$Ca_3(PO_4)_2$ has been found by the XRD study. At 1,100 °C the maximal content of YPO_4 in the solid solution is ~15 mass% (~23 mol%).

The existence of the limited solid solutions at high temperatures has been evidenced by the observed temperature change of β→α and α→α′ transitions. The limited solid solutions with the α and α′-$Ca_3(PO_4)_2$ structure exist in narrowed phase fields in comparison to the β phase. The maximal doping of the α solid solution with *RE* amounts to ~3 mass%. This may not be sufficient active ion content in the α phase necessary to achieve a long-lasting phosphorescence or to apply the material in thermoluminescence dosimetry [47].

There are several similarities between the $Ca_3(PO_4)_2$–YPO_4 and $Ca_3(PO_4)_2$–$CePO_4$ systems [36]. Despite the difference between the $CePO_4$ (monazite) and YPO_4 structures (xenotime), concentration and temperature ranges of all phases in the systems are close to each other.

Conclusions

The phase diagram of the $Ca_3(PO_4)_2$–YPO_4 system has been proposed in the revised form. The presented results confirm existence of three fields of limited solid solution with β, α-, and α′-$Ca_3(PO_4)_2$ structure. At 1,100 °C the single-phase field of the YPO_4 solid solution in β-$Ca_3(PO_4)_2$ extends to ~15 mass% (~23 mol%). The high-temperature solid solutions form in narrowed concentration range in comparison to the β phase.

The doping by YPO_4 results in easier α→β transformation than in pure $Ca_3(PO_4)_2$. The metastable α solid solution can be obtained only by quenching of samples with the low YPO_4 content. Since the doped material crack on cooling, obtaining of dense ceramic with the α structure is not possible.

The $Ca_3Y(PO_4)_3$ phosphate is a thermodynamically stable phase at temperature exceeding 1,255 °C, and it has one structural form.

References

1. Bohner M. Calcium orthophosphates in medicine: from ceramics to calcium phosphate cements. Injury. 2000;36:SD37–47.
2. LeGeros RZ. Properties of osteoconductive biomaterials: calcium phosphates. Clin Orthop Relat Res. 2002;395:81–9.
3. Troemel G, Harkortz HJ, Hotop W. Untersuchungen im System CaO–P_2O_5–SiO_2 Z. Anorg Chem. 1948;256:253–72.
4. Nurse RW, Welch JH, Gutt W. A new form of tricalcium phosphate. Nature. 1958;182:1230.
5. Yashima M, Sakai A. High-temperature neutron powder diffraction study of the structural phase transition between α and α′ phases in tricalcium phosphate $Ca_3(PO_4)_2$. Chem Phys Lett. 2003;372:779–83.
6. Welch JH, Gutt W. High-temperature studies of system calcium oxide-phosphorus pentoxide. J Chem Soc. 1961;4442–4.
7. Barin I. Thermochemical data of pure substances. Part I–II. Weinheim: VCH Verlags Gesellschaft; 1993.
8. Carrodeguas RG, De Aza A H, Turrillas X, Pena P, De Aza S. New approach to the β → α polymorphic transformation in Magnesium-substituted Tricalcium Phosphate and its practical implications. J Am Ceram Soc. 2008;91:281–6.
9. Mathew M, Schroeder LW, Dickens B, Brown WE. The crystal structure of α-$Ca_3(PO_4)_2$. Acta Crystallogr B. 1977;33:1325–33.
10. Fuierer TA, Lore M, Puckett SA, Nancollas GH. A mineralization adsorption and mobility study of hydroxyapatite surfaces in the presence of zinc and magnesium ions. Langmuir. 1994;10:4721–5.
12. Dickens B, Schroeder LW, Brown WE. Crystallographic studies of the role of Mg as a stabilizing impurity in β-$Ca_3(PO_4)_2$. The crystal structure of pure β-$Ca_3(PO_4)_2$. J Solid State Chem. 1974;10:232–48.
13. Yashima M, Sakai A, Kamiyama T, Hoshikawa A. Crystal structure analysis of β-tricalcium phosphate $Ca_3(PO_4)_2$ by neutron powder diffraction. J Solid State Chem. 2003;175:272–7.
14. Kannan S, Goetz-Neunhoeffer F, Neubauer J, Ferreira JMF. Cosubstitution of zinc and strontium in β-tricalcium phosphate: synthesis and characterization. J Am Ceram Soc. 2011;94:230–5.

15. Golubev VN, Lazoryak BI. Double phosphates $Ca_9R(PO_4)_7$ (R = Rare earth element, Y, Bi) with the whitlockite structure. Inorg Mater. 1991;27480–3.
16. Lazoryak BI, Golubev VN, Salmon R, Parent C, Hagenmuller P. Distribution of Eu^{3+} ions in whitlockite-type $Ca_{3-x}Eu_{2x/3}(PO_4)_2$ orthophosphates. Eur J Solid State Inorg Chem. 1989;26:455–63.
17. Bessiere A, Benhamou RA, Wallez G, Lecointre A, Viana B. Site Occupancy and mechanisms of thermally stimulated luminescence in $Ca_9Ln(PO_4)_7$ (Ln = lanthanide). Acta Mater. 2012;60:6641–9.
18. Du F, Nakai Y, Tsuboi T, Huang Y, Seo HJ. Luminescence properties and site occupations of Eu^{3+} ions doped in double phosphates $Ca_9R(PO_4)_7$ (R = Al, Lu). J Mater Chem. 2011;21:4669–77.
19. Lecointre A, Bessiere A, Viana B, Ait Benhamou R, Gourier D. Thermally stimulated luminescence of $Ca_3(PO_4)_2$ and $Ca_9Ln(PO_4)_7$ (Ln = Pr, Eu, Tb, Dy, Ho, Er, Lu). Radiation Meas. 2010;45:273–6.
20. Bessiere A, Lecointre A, Ait Benhamou R, Suard E, Wallez G, Viana B. How to induce red persistent luminescence in biocompatible $Ca_3(PO_4)_2$. J Mater Chem C. 2013;1:1252–9.
21. Suchanek W, Yoshimura M. Processing and properties of hydroxyapatite-based biomaterials for use as hard tissue replacement implants. J Mater Res. 1998;13:94–117.
22. Cuneyt Tas A, Bhaduri S, Jalota S. Preparation of Zn-doped β-tricalcium phosphate (β-$Ca_3(PO_4)_2$) bioceramics. Mater Sci Eng C. 2007;27:394–401.
23. Yoshida K, Kondo N, Kita H, Mitamura M, Hashimoto K, Toda Y. Effect of substitutional monovalent and divalent metal ions on mechanical properties of β-tricalcium phosphate. J Am Ceram Soc. 2005;88:2315–8.
24. Bucur AI, Bucur R, Vlase T, Doca N. Thermal analysis and high-temperature X-ray diffraction of nano-tricalcium phosphate crystallization. J Therm Anal Calorim. 2012;107:249–55.
25. Tonsuaadu K, Gross KA, Pluduma L, Veiderma M. A review on the thermal stability of calcium apatites. J Therm Anal Calorim. 2012;110:647–59.
26. Chatzistavrou X, Zorba T, Chrissafis K, Kaimakamis G, Kontonasaki E, Koidis P, Paraskevopoulos KM. Influence of particle size on the crystallization process and the bioactive behavior of a bioactive glass system. J Therm Anal Calorim. 2006;85:253–9.
27. Nagai M, Shibuya Y, Nishino T, Saeki T, Owada H, Yamashita K, Umegaki T. Electrical conductivity of calcium phosphate ceramics with various Ca/P ratios. J Mater Sci. 1991;26:2949–53.
28. Wang W, Itoh S, Yamamoto N, Okawa A, Nagai A, Yamashita K. Electrical polarization of β-tricalcium phosphate ceramics. J Am Ceram Soc. 2010;93:2175–7.
29. Teterskii AV, Yu S, Stefanovich V, Lazoryak BI, Rusakov DA. Whitlockite solid solutions $Ca_{9-x}M_xR(PO_4)_7$ ($x = 1$, 1.5; M = Mg, Zn, Cd; R = Ln, Y) with antiferroelectric properties. Rus J Inorg Chem. 2007;52:308–14.
30. Enderle R, Gotz-Neunhoeffer F, Goebbels M, Mueller FA, Greil P. Influence of magnesium doping on the phase transformation temperature of β-TCP ceramics examined by Rietveld refinement. Biomaterials. 2005;26:3379–84.
31. Aldred AT. Cell volumes of APO_4, AVO_4, and $ANbO_4$ compounds, where A = Sc, Y La–Lu. Acta Crystallogr. 1984;B40:569–74.
32. Hikichi Y, Nomura T. Melting temperatures of monazite and xenotime. J Am Ceram Soc. 1987;70:C252–3.
33. Szuszkiewicz W, Znamierowska T. Phase equilibria in the system Y_2O_3–P_2O_5. Pol J Chem. 1989;63:381–91.
34. Szuszkiewicz W, Znamierowska T. The system YPO_4–$Ca_3(PO_4)_2$. J Solid State Chem. 1990;88:406–10.
35. Jungowska W. The system $Ca_3(PO_4)_2$–$LaPO_4$. Solid State Sci. 2002;4:229–32.
36. Matraszek A, Szczygieł I. Phase relationships in the tricalcium phosphate–cerium phosphate system. Thermal behavior of phases present in the system. J Am Ceram Soc. 2012;95:3651–6.
37. Bandrowski S, Znamierowska T. Investigation of phase equilibria in the Er_2O_3–Na_2O–P_2O_5 system: the partial system $ErPO_4$–$NaPO_3$–$Er(PO_3)_3$. J Therm Anal Calorim. 2013;113:105–11.
38. Piotrowska D, Znamierowska T, Szczygieł I. Phase equilibria in the $ErPO_4$–K_3PO_4 system. J Therm Anal Calorim. 2013;113:121–6.
39. Szuszkiewicz W, Radominska E, Znamierowska T, Wilk P. Phase equilibria in the YPO_4–Rb_3PO_4 system. J Therm Anal Calorim. 2013;111:63–9.
40. McCarthy GJ, Pfoertsch DE. $Ca_3Ln(PO_4)_3$ (Ln = La–Gd) phases with the eulityte structure. J Solid State Sci. 1981;38:128–9.
41. Fukuda K, Iwata T, Niwa T. Crystal structure and phase transformations of calcium yttrium orthophosphate, $Ca_3Y(PO_4)_3$. J Solid State Chem. 2006;179:3420–8.
42. Berak J, Znamierowska T. Phase equilibria in system CaO–Na_2O–P_2O_5. 4. Partial system CaO–$Ca_2P_2O_7$–Na_2O. Roczniki Chemii. 1973;47:1137–48.
43. Laugier J, Bochu B. LMGP-Suite of Programs for the Interpretation of X-ray Experiments, ENSP Laboratoire des Materiaux et du Genie Physique, BP. France: Saint Martin d'Heres; 2004.
44. Shannon RD. Revised effective ionic radii and systematic studies of interatomic distances in halides and chalcogenides. Acta Crystallogr. 1972;A32:751–67.
45. Matraszek A. Study of phase relationships in the $Sr_3(PO_4)_2$–$CePO_4$ system. Phase diagram and thermal characteristics of phases. J Solid State Chem. 2013;203:86–91.
46. Rycerz L. Practical remarks concerning phase diagrams determination on the basis of differential scanning calorimetry measurements. J Therm Anal Calorim. 2013;113:231–8.
47. Ait Benhamou R, Bessiere A, Wallez G, Viana B, Elaatmani M, Daoud M, Zegzouti A. New insight in the structure-luminescence relationships of $Ca_9Eu(PO_4)_7$. J Solid State Chem. 2009;182:2319–25.